

Carbon nanotubes of polyethylene

E.F. Kukovitskii ^a, L.A. Chernozatonskii ^b, S.G. L'vov ^a, N.N. Mel'nik ^c

^a *Kazan Physical-Technical Institute, Kazan 420029, Russian Federation*

^b *Institute of Chemical Physics, Moscow 117334, Russian Federation*

^c *Lebedev Physical Institute, Moscow 117924, Russian Federation*

Received 16 December 1996

Abstract

Crooked carbon nanotubes 10–40 nm in diameter were obtained at 420–450°C by the pyrolysis of granular polyethylene in a helium atmosphere using a Ni plate as catalyst. Production of this powder was 200–300 mg per hour. Their identification was made by transmission electron microscopy, Raman spectroscopy, electron and X-ray diffraction. The oxidation reaction of the nanotube powder has been studied and compared to the oxidation of polycrystalline graphite and arc-processed multi-shell nanotubes.

1. Introduction

Tubular derivatives of fullerenes have become a topic of extensive experimental and theoretical investigations. Single-shell carbon nanotubes can be prepared by co-evaporating iron, cobalt or nickel (catalysts) during a carbon arc-discharge [1,2]. This was a new development in carbon research, since multi-shell tubules are formed at the tip of the cathode inside cigar-like deposits under normal conditions (no catalysts) [3,4] as well as at solid substrates under conditions of high-density carbon flow in at vacuum [5,6]. The main limitations of the arc-discharge process are its low yield that makes the product expensive. The catalytic production method is simpler and more reproducible than the arc-discharge one. It has been known for some time that filamentous carbon may be produced by the pyrolysis of hydrocarbons, and the growth of hollow carbon filaments during pyrolysis in the presence of

metal particles was described earlier [7–10]. The fibres grow from various substrates heat-treated from 300 to 1100°C in atmospheres containing either carbon monoxide or hydrocarbon gases. The starting materials used in previous studies include such compounds as benzene, methane, ethylene, acetylene and carbon monoxide. Unfortunately, the catalytically fabricated tubules are usually thicker than those obtained by an arc-discharge process and often appear in a mixture with amorphous carbon and graphite. The future of catalytically grown carbon fibres with diameters up to ≈ 100 nm depends on how one can isolate the fibres from the catalyst particles and soot that are co-deposited in the synthesis process. Because of recent interest in mesoscopic systems consisting of clusters of atoms 1–100 nm in size and possessing physical properties between the molecular and bulk solid state limit, the macroscopic quantities of carbon nanotubes are required for academic studies and applications.

2. Synthesis and structure investigations

In this work we have obtained microsize crooked carbon fibres by the catalytic pyrolysis of granular polyethylene in helium atmosphere using a nickel plate as catalyst. The nickel plate was located in a quartz reactor which was heated from the outside by a nichrome element. The most representative conditions were as follows: total pressure 4 atmosphere,

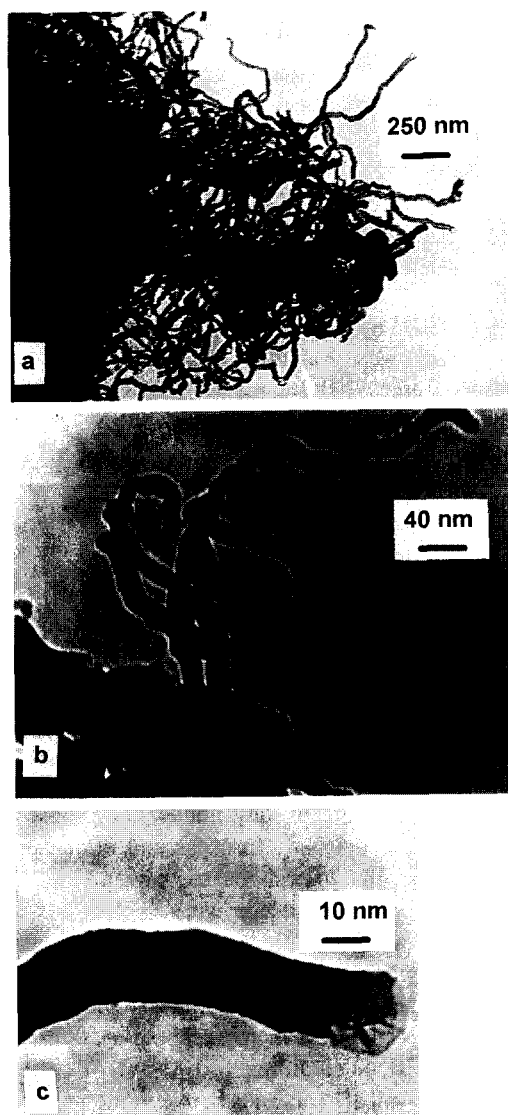


Fig. 1. TEM images of the synthesised carbon material: (a) fibre clew with Ni nanoparticles (dark spots); (b) some tubes grown on a Ni particle; (c) the end of the single tube.

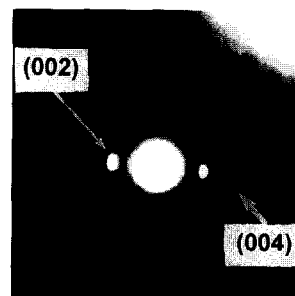


Fig. 2. Electron diffraction pattern from the single nanotube shown in Fig. 1c. Diffraction spots are streaked toward the direction normal to the tube axis. Arrows show selected areas of spots.

temperature 420–450°C, reaction time 50–60 min, the yield of carbon being $\approx 3 \times 10^{-3}$ g/cm² per hour.

The morphology, some structure characteristics and thermal oxidation in the air of the material obtained have been examined. Fig. 1 presents transmission electron micrographs showing the typical appearance of the carbonaceous deposit with the major constituent being filamentous carbon. From observation in many experiments the range of fiber diameters 10–40 nm was determined with a few extremely thick fibres about 100 nm in diameter. Clear evidence of the fact that many carbonaceous filaments are crooked tubes is presented in the electron micrographs in Figs. 1b and 1c. The central hollow channel was determined to be about 2–4 nm in diameter.

A considerable body of information concerning this type of carbonaceous tube has been built up over the last two decades, but the details of the growth mechanism for various observed tube shapes are only now being discussed [10,11]. Catalytic particles are involved in this mechanism, and they help to determine the cross section of the tubes. Such particles, opaque for electrons, can be seen at the head of the filaments and are identified as nickel particles by X-ray diffraction data. The diameters of the filaments were frequently but not always the same as those of the particles at their head. Sometimes these particles are not encapsulated by a catalytic carbon deposit; in other cases they are covered by carbon layers. It is also evident from a micrograph (Fig. 1b) that active nickel particles may be responsible for the

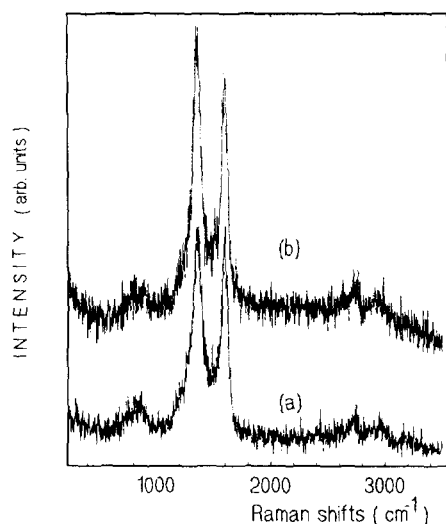


Fig. 3. Raman spectra of the obtained carbon material: (a) deposit on a Ni plate; (b) powder scraped off the Ni substrates.

growth of more than one filament in contradiction to previous observations [7,10].

An electron diffraction pattern from a single nanotube is shown in Fig. 2. The (002) reflections are relatively strong in intensity and form two diffuse spots (for a straight segment of the tube) at diametrically opposite points. Weak (004) reflections are also seen in the micrograph. The (001) spots are due to Bragg reflections from graphitic layers parallel to the incident beam. The spacing between the graphitic sheets (d_{002}) measured from (001) diffraction patterns is 0.344 nm, wider by a few percent than that of an ideal graphite crystal (0.3354 nm). The wide interplanar spacing is characteristic of the turbostratic carbon. The (001) reflections spread into areas $\approx 20^\circ$, and the disorientation of atomic layers should be equal to this value. The ($hk0$) rings are brought about by graphite sheets perpendicular to the incident beam. The character of the (100) and (110)

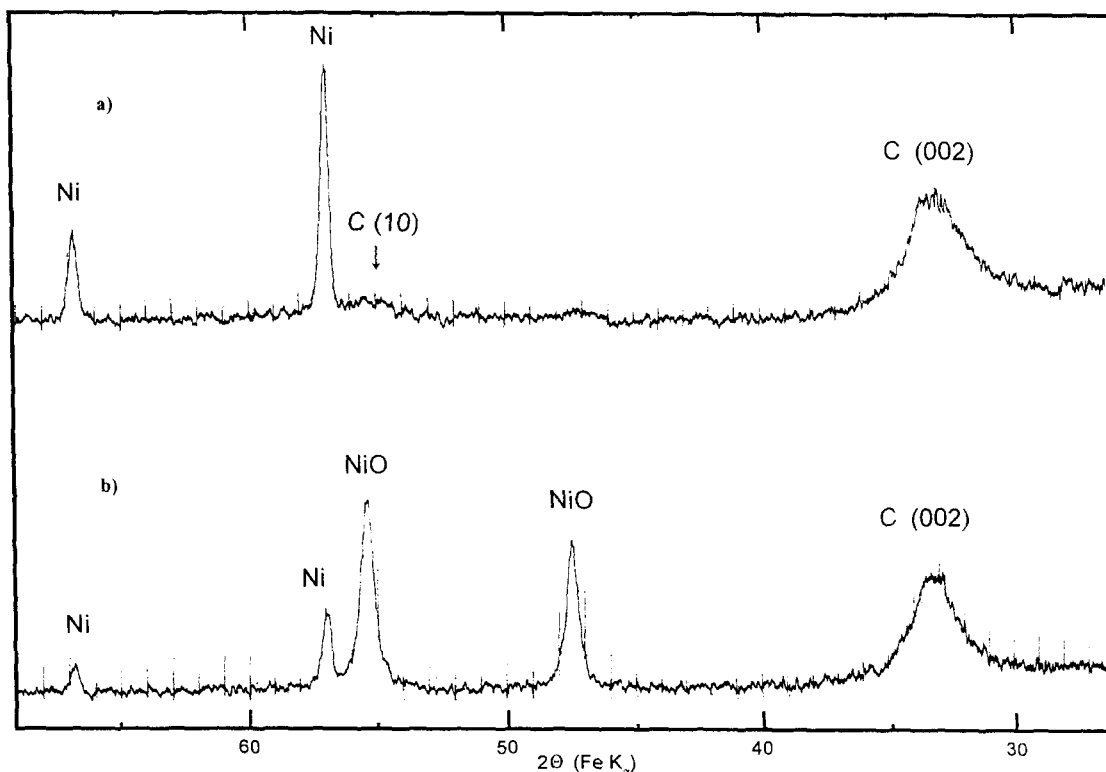


Fig. 4. X-ray diffraction patterns of the synthesised material (a), and the same after heating up to 50% weight loss (b). The Ni content in samples under investigation was established to be 10–20% according to the wet chemical analysis.

reflections (the intensity distributed on rings) indicates that the stacking of graphite sheets is disordered (so-called turbostratic stacking). In accordance with the described diffraction picture for a single tube the electron diffraction patterns for agglomerations of tubes are typical of the two-dimensional layer structure (turbostratic structure): only (hk) patterns present a part of the (001) reflections, and they have a characteristic asymmetric form with a tail on the larger radius side. They are representative patterns of fibres in which all carbon layers are roughly parallel to the fibre axis, but in which the a axes of the stacks are randomly oriented. The situation as a whole is analogous to that of carbon filaments grown by decomposition of other hydrocarbon materials [7–10].

Raman spectra of our carbon deposited directly on a Ni plate (Fig. 3a) and of the deposit powder (Fig. 3b) were measured at room temperature with the 5145 Å line of an argon ion laser in the frequency range from 200 to 3500 cm^{-1} . They include two first-order broad high intensity bands centred at 1350 and 1590 cm^{-1} , and a weak peak near 830 cm^{-1} . We also see broad bands of second-order features near 2650 and 2950 cm^{-1} . The spectra are close to those of a multi-shell tube containing soot obtained by the carbon arc method [12], which confirms TEM investigations.

For the purpose of obtaining a better understanding of the microscopic structure, X-ray diffraction (using $\text{Fe K}\alpha$ radiation) was performed for the synthesised material (Fig. 4). The maximum position of a broad (002) diffraction peak of turbostratic carbon coincides approximately with that of graphite, which provides 0.34 nm of interlayer spacing in accordance with electron diffraction data. A weak (10) turbostratic reflection is also seen at the angle $2\theta \approx 55^\circ$. Two strong peaks belong to pure nickel seen as small particles on the electron micrographs. Therefore, the structure study establishes the synthesised filamentous carbon to be a special in situ nanocomposite material consisting mainly of carbon nanotubes with nickel nanoparticles at their tips.

3. Oxidation

Recently, some efforts were made to modify capped hollow carbon nanotubes into nanocomposite

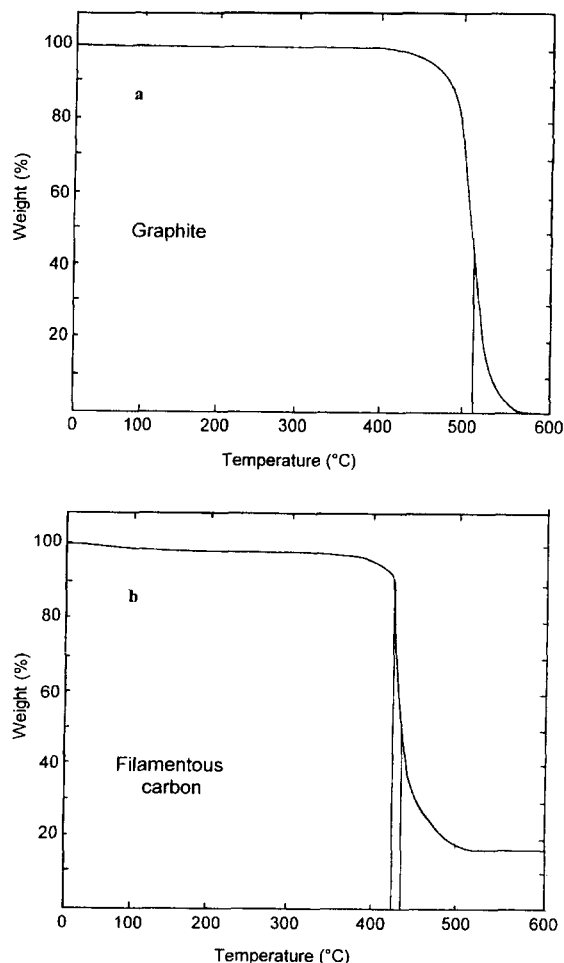


Fig. 5. Weight loss experiments under heating of polycrystalline graphite (a), and the synthesised carbon material (b).

fibres by heating the tubes in the presence of air and filling of the interior with a metal [13,14]. In this connection, a better understanding is needed of the oxidation mechanism for carbon of such a specific morphology. The oxidation of obtained carbonaceous deposit has been studied by thermogravimetric experiments. Approximately 10 mg of the material was heated in an open platinum pan in the air. The oxidation was performed at the constant rate of weight loss 0.4 mg/min. Results are shown in Fig. 5 for filamentous carbon and typical graphite. It is clear from the observation that the oxidation of the filamentous material occurs at a temperature (\approx

420°C) which is lower than the temperature, at which basic graphite planes react with oxygen ($\approx 520^\circ\text{C}$). It is also much lower than the oxidation temperature of nanotubes obtained by the arc process [13,14], which show a high resistance to oxidation up to 750°C in the air. The shapes of the curves are essentially different for graphite and filamentous carbon. The weight loss for graphite is accompanied by an increase in temperature in the range 480–540°C. In contrast to graphite, filamentous carbon loses up to 50–60% of its starting weight within the narrow temperature interval of 5–7°C followed by a wide temperature range (440–500°C) to complete the sample oxidation. The different kinetics of the oxidation reaction for filamentous carbon point to the fact that more than one form of carbon is present in the samples under investigation or maybe another carbonaceous “phase” arises due to incomplete oxidation of the starting material. The state of the partially (50–60% weight loss) oxidised samples was investigated using a transmission electron microscope, revealing that the oxidation reaction causes complete disintegration of the carbon fibres (Fig. 5b). Electron diffraction of the “coarse-grained” residue of the samples reveals only graphite rings, which indicate a somewhat more graphitized carbon as compared to electron diffraction patterns of fibres. Powder X-ray diffraction data for the heated material confirm this observation by a decrease in the (002) line half-peak width and interplanar spacing d_{002} to the value of 0.338 nm. Scherrer’s equation for the correlation between linewidth and crystal size yields a crystal size along the c direction (L_c) of 60 Å. One can infer that the final stage of the thermogravimetric analysis relates to oxidation of carbonaceous material with turbostratic-like structure, the number of layers in the unit cell being ≈ 20 . Oxidation of this carbon occurs at temperatures approaching that of graphite oxidation.

The initial stage of the oxidation reaction should therefore be attributed to pure filamentous carbon. One would expect that the low onset temperature of the oxidation is determined by a highly defective surface structure of fibres consisting of turbostratic stacks of carbon layers parallel to the fibre axis. It is well known that terminated graphitic planes provide highly reactive centres which can initiate oxidation reactions.

4. Conclusions

The tips of fibres are an important source of active centres. Recent experiments on opening carbon nanotubes show that the tips of the tubes react first with oxygen and that the tips curvature, and thus the strain, must be a key factor in the onset of oxidation at nanotube tips [14]. Most catalytically grown fibres contain small particles of nickel at their tips. The oxidation reaction may be catalysed either by metallic nickel or nickel oxide arising in the heating process. Fig. 4b shows that synthesised carbon contains a crystalline form of nickel oxide after heating up to 50% weight loss and almost complete “burning” of fibres. The intensity of the metallic nickel reflections is, at the same time, much dropped. This indicates that nickel particles do oxidise at an early stage of the oxidation process and might help to initiate the reaction and to lower the onset temperature. It should be mentioned that previous experiments with arc-processed carbon nanotubes in air demonstrated that the onset of the oxidation reaction shifted to lower temperatures in samples containing lead oxide [11]. In the presence of metal lead, the opening of tubes occurs at a much lower temperature ($\approx 400^\circ\text{C}$) as compared to pure carbon nanotubes ($\approx 750^\circ\text{C}$) [13,14]. It was proposed that the oxidation reaction must have been catalysed either by lead particles or by some form of lead oxide. More thorough experiments and analyses are needed to elucidate the details of the oxidation mechanism of carbon nanotubes in the presence of various metals. Such studies may fall within the realms of low-dimensional chemistry.

Acknowledgement

This work is supported by the ISTC (grant N 079) and the Russian Program of “Fullerenes and Atomic Clusters” (grant N 94004).

References

- [1] S. Iijima and T. Ichihashi, *Nature* 363 (1993) 603.
- [2] D.S. Bethune, C.H. Kiang, M.S. de Vries, G. Gorman, R. Savoy, J. Vazquez and R. Beyers, *Nature* 363 (1993) 605.

- [3] S. Iijima, *Nature* 354 (1991) 56.
- [4] T.W. Ebbesen and P.M. Ajayan, *Nature* 368 (1992) 220.
- [5] M. Ge and K. Settler, *Science* 260 (1993) 515.
- [6] L.A. Chernozatonskii, Z.Ya. Kosakovskaya, A.N. Kiselev and N.A. Kiselev, *Chem. Phys. Lett.* 228 (1994) 94.
- [7] R.T.K. Barker, M.A. Barber, P.S. Harris, F.S. Feates and R.J. Waite, *J. Catal.* 26 (1972) 51.
- [8] A. Oberlin, M. Endo and T. Koyana, *J. Cryst. Growth* 32 (1976) 335.
- [9] M. Jose-Yacaman, M. Miki-Yoshida, L. Rendou and J.S. Santiesteban, *Appl. Phys. Lett.* 62 (1993) 657.
- [10] V. Ivanov, J.B. Nagy, Ph. Lambin, A. Lucas, X.B. Zhang, X.F. Zhang, D. Bernaerts, G. Van Tendeloo, S. Amelinckx and J. Van Landuyt, *Chem. Phys. Lett.* 223 (1994) 329.
- [11] P.M. Ajayan and S. Iijima, *Nature* 361 (1993) 333.
- [12] R.A. Jishi, L. Venkataraman, M.S. Dresselhaus and G. Dresselhaus, *Chem. Phys. Lett.* 209 (1993) 77.
- [13] S.C. Tsang, P.J.F. Harris and M.L.H. Green, *Nature* 362 (1993) 522.
- [14] P.M. Ajayan, T.W. Ebbesen, T. Ichihashi, K. Tanigaki and H. Hiura, *Nature* 362 (1993) 522.